

Syntheses, Reactivity, and Stereochemistry of η^3 -Allyl Dithio-Molybdenum Complexes: Crystal Structures of *endo*-[Mo(η^3 -C₃H₅)(η^2 -S₂CNC₄H₈)(CO)(η^2 -dppe)], *endo*-[Mo(η^3 -C₃H₅){ η^2 -S₂P(OEt)₂}(CO)(η^2 -dppe)], *exo*-, *endo*-[Mo(η^3 -C₃H₅)(η^2 -S₂CNC₄H₈)(CO)(η^2 -dppm)], and *endo*-[Mo(η^3 -C₃H₅){ η^2 -S₂P(OEt)₂}(CO)(η^2 -dppm)]

Kuang-Hway Yih,^{*,†} Gene-Hsiang Lee,[‡] Shou-Ling Huang,[‡] and Yu Wang[§]

Department of Applied Cosmetology, Hung Kuang Institute of Technology, Shalu, Taichung Hsien, Taiwan 433, Republic of China, Instrumentation Center, College of Science, National Taiwan University, Taipei, Taiwan 106, Republic of China, and Department of Chemistry, National Taiwan University, Taipei, Taiwan 106, Republic of China

Received September 3, 2002

The reactions of η^3 -allyldicarbonyldithiomolybdenum(II) compounds [Mo(η^3 -C₃H₅)(CO)₂(η^2 -L₂)(X)] (L₂, X = S₂CNC₄H₈ (**1a**); S₂CN₂Et₂ (**1b**); S₂P(OEt)₂, CH₃CN (**1c**)) with diphos in refluxing acetonitrile give a mixture of *endo* and *exo* complexes [Mo(η^3 -C₃H₅)(η^2 -L₂)(CO)(η^2 -diphos)] (diphos: dppe = {1,2-bis(diphenylphosphino)ethane} (**2–4**); dppm = {bis(diphenylphosphino)methane} (**5–7**); dppa = {bis(diphenylphosphino)amine} (**8–10**)). The orientations of *endo* and *exo* are defined for the open face of the allyl group and carbonyl group in the same direction in the former and opposite directions in the latter. In solution, both the *endo* and the *exo* isomers are present in dithiocarbamate Mo complexes, whereas only the *endo* conformer is present in dithiophosphate dppe and dppa Mo complexes. The variable-temperature ¹H and ³¹P{¹H} NMR experiments and X-ray crystal structures of *endo*-[Mo(η^3 -C₃H₅)(η^2 -S₂CNC₄H₈)(CO)(η^2 -dppe)] (**2**), *endo*-[Mo(η^3 -C₃H₅){ η^2 -S₂P(OEt)₂}(CO)(η^2 -dppe)] (**4**), *exo*- and *endo*-[Mo(η^3 -C₃H₅)(η^2 -S₂CNC₄H₈)(CO)(η^2 -dppm)] (**5**), and *endo*-[Mo(η^3 -C₃H₅){ η^2 -S₂P(OEt)₂}(CO)(η^2 -dppm)] (**7**) are used to elucidate the allyl rotation mechanism and the two orientations. The activation barriers of interconversion were determined to be 61.5 ± 0.4 (**3**) and 65.1 ± 0.4 kJ mol⁻¹ (**5**). X-ray analysis on **5** shows that the unit cell contains two independent molecules, *endo* and *exo*, which differ mainly by the orientation of the allyl group with respect to the carbonyl group. This is the first example of such a conformation in the crystal structure of the Mo(η^3 -C₃H₅)(η^2 -L) derivative.

Introduction

In discussing stereochemical nonrigidity in complexes [CpMo(CO)₂(η^3 -allyl)]¹ and [(L₃)Mo(CO)₂(η^3 -allyl)]² (L₃: Tp = hydrotris(pyrazolyl)borate or Tp' = hydrotris(3,5-dimethylpyrazolyl)borate), the nonrigidity is often attributed to rotation of the allyl group about the metal- η^3 -allyl axis in the former (*endo*/*exo* orientation) and to a trigonal twist of the tridentate ligand or a η^3 - η^1 - η^3 interconversion³ of the allyl group in the latter.

The fluxionality^{4,13b} and X-ray crystallography⁵ of complexes containing the [Mo(η^3 -allyl)(CO)₂(η^2 -A)X] (A

* Address correspondence to this author. E-mail: khyih@sunrise.hkc.edu.tw. FAX: 886-4-26321046. Phone: 886-4-26318652-ext-5308.

[†] Hung Kuang Institute of Technology.

[‡] College of Science, National Taiwan University.

[§] Department of Chemistry, National Taiwan University.

(1) (a) King, R. B. *Inorg. Chem.* **1966**, *5*, 2242. (b) Davison, A.; Rode, W. C. *Inorg. Chem.* **1967**, *6*, 2124. (c) van Staveren, D. R.; Weyhemüller, T.; Metzler-Nolte, N. *Organometallics* **2000**, *19*, 3730 and references therein.

(2) (a) Trofimenko, S. *J. Am. Chem. Soc.*, **1969**, *91*, 3183. (b) Faller, J. W.; Haitko, D. A.; Adams, R. D.; Chodosh, D. F. *J. Am. Chem. Soc.* **1977**, *99*, 1654. (c) Faller, J. W.; Haitko, D. A.; Adams, R. D.; Chodosh, D. F. *J. Am. Chem. Soc.* **1979**, *101*, 865. (d) Ward, Y. D.; Villanueva, L. A.; Allred, G. D.; Payne, S. C.; Semones, M. A.; Liebeskind, L. S. *Organometallics* **1995**, *14*, 4132.

(3) (a) Chowdhury, S. K.; Nandi, M.; Joshi, V. S.; Sarkar, A. *Organometallics* **1997**, *16*, 1806 and references therein. (b) Kollmar, M.; Goldfuss, B.; Reggelin, M.; Rominger, F.; Helmchen, G. *Chem. Eur. J.* **2001**, *7*, 4913.

(4) (a) Graham, A. J.; Fenn, R. H. *J. Organomet. Chem.* **1969**, *17*, 405. (b) *J. Organomet. Chem.* **1970**, *25*, 173. (c) Cotton, F. A.; Frenz, B. A.; Stanislawski, A. G. *Inorg. Chim. Acta* **1973**, *7*, 503. (d) Dewans, F.; Dewailly, J.; Meunier-Piret, J.; Piret, P. *J. Organomet. Chem.* **1974**, *76*, 53.

(5) (a) Fenn, R. H.; Graham, A. J. *J. Organomet. Chem.*, **1972**, *37*, 137. (b) Graham, A. J.; Akrigg, D.; Sheldrick, B. *Cryst. Struct. Commun.* **1976**, *24*, 173. (c) Cotton, F. A.; Murillo, C. A.; Stults, B. R. *Inorg. Chim. Acta* **1977**, *7*, 503. (d) Cosky, C. A.; Ganis, P.; Avatibile, G. *Acta Crystallogr., Sect. B* **1971**, *B27*, 1859. (e) Faller, J. W.; Chodosh, D. F.; Katahira, D. *J. Organomet. Chem.* **1980**, *187*, 227. (f) Cotton, F. A.; Jeremic, M.; Shaver, A. *Inorg. Chim. Acta* **1972**, *6*, 543.

(6) Curtis, M. D.; Eisenstein, O. *Organometallics* **1984**, *3*, 887. (7) Espinet, P.; Hernandez, R.; Iturbe, G.; Villafaña, F.; Orpen, A. G.; Pascual, I. *Eur. J. Inorg. Chem.* **2000**, 1031.

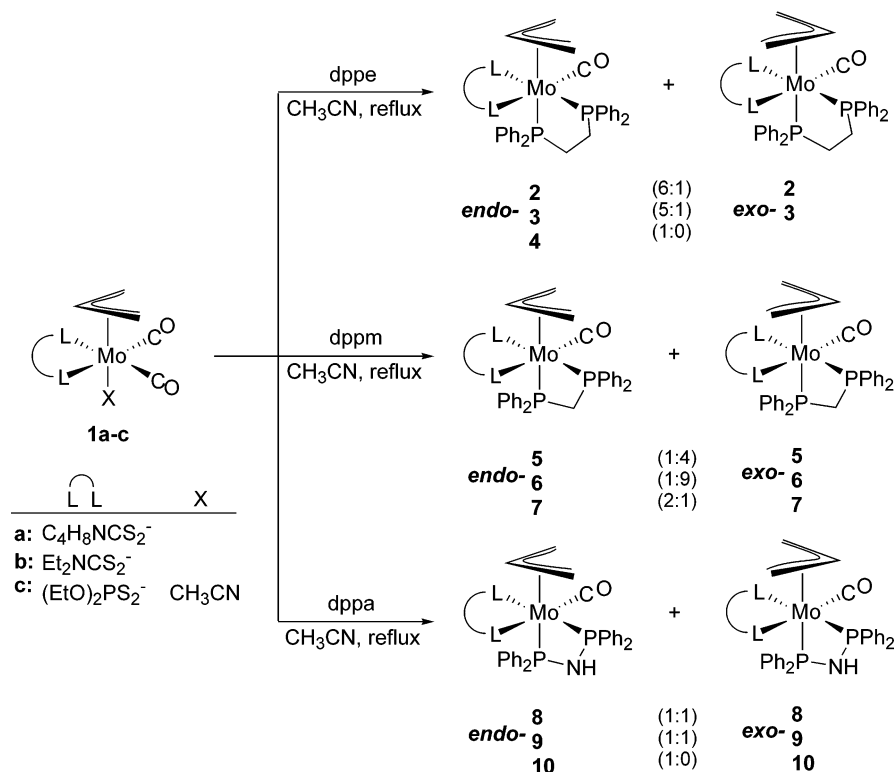
(8) Faller, J. W.; Lambert, C.; Mazzieri, M. R. *J. Organomet. Chem.* **1990**, *383*, 161.

(9) Yih, K. H.; Lee, G. H.; Wang, Y. *Inorg. Chem. Commun.* **2000**, *3*, 458.

(10) Shiu, K. B.; Yih, K. H.; Wang, S. L.; Liao, F. L. *J. Organomet. Chem.* **1991**, *420*, 359.

(11) Yih, K. H.; Lee, G. H.; Wang, Y. *J. Organomet. Chem.* **1999**, *588*, 125.

Scheme 1



= pyrazolylborate, β -diketonate, dithiocarbamate, X = neutral monodentate ligand; A = diphos, pyridylphosphane, X = halide) type have also been well investigated as an intramolecular trigonal twist. The most important result is that, for each Mo atom discussed above, when the coordinated η^3 -allyl group adopted a conformation that placed the open face of the allyl group toward the adjacent cis (CO)₂ grouping, an electronic stabilization⁶ for this particular orientation is indicated. A novel pivoted double switch⁷ and pyridyl-exchange mechanism have been reported when the A ligands were replaced by pyridylphosphane or their oxides ligands. Notably, previously no allyl rotation or rearrangement involving a π - σ - π process has been reported for the $[\text{Mo}(\eta^3\text{-allyl})(\text{CO})_2(\eta^2\text{-A})\text{X}]$ derivatives.

The rigid cyclopentadienyl crystal structures of both *endo*- and *exo-cis-syn*- $[\text{CpMo}(\text{NO})(\text{CO})\{\eta^3\text{-CH}(\text{Ph})\text{-CHCH}_2\}] [\text{BF}_4]$ have been reported by Faller et al.⁸ In addition, we have previously studied the *endo* and *exo* complexes of $[\text{Mo}(\eta^3\text{-C}_3\text{H}_5)\{\eta^2\text{-S}_2\text{P}(\text{OEt})_2\}(\text{CO})(\eta^2\text{-dppm})]$ from ³¹P{¹H} NMR spectra.⁹ On the other hand, clear crystal structures of these two conformations and the fluxional behavior of complexes including the $[\text{Mo}(\eta^3\text{-C}_3\text{H}_5)(\eta^2\text{-A})(\text{CO})(\eta^2\text{-A})]$ type are much less studied.

In this work we describe the syntheses of diphos derivatives of **1a-c** and their allyl rotation interconversion along with spectroscopic and crystal structures investigations. The first crystallographic evidence for the *endo*- and *exo*-allyl ligand in $[\text{Mo}(\eta^3\text{-C}_3\text{H}_5)(\eta^2\text{-dithio})(\text{CO})(\eta^2\text{-diphos})]$ derivatives is presented.

Result and Discussion

Syntheses. A convenient way of preparing dithioallyl complexes of the type $[\text{Mo}(\eta^3\text{-C}_3\text{H}_5)(\text{CO})_2(\eta^2\text{-L}_2)(\text{X})]$ (L_2 , X = $\text{S}_2\text{CNC}_4\text{H}_8$ (**1a**);¹⁰ S_2CNET_2 (**1b**);¹⁰ $\text{S}_2\text{P}(\text{OEt})_2$, CH_3CN (**1c**)¹¹) is via the reaction of complex $[\text{Mo}(\eta^3\text{-C}_3\text{H}_5)(\text{CO})_2(\text{CH}_3\text{CN})_2(\text{Br})]$ and the dithio ligands in acetonitrile at room temperature. Reactive η^3 -allyldithiocarbonyldithiomolybdenum(II) complexes having one vacant (**1a,b**) or one pseudovacant (**1c**) coordination site at the molybdenum center are due to the unsaturated 16-electron complexes and one labile acetonitrile solvate complex. Facile coordinative or substituted compounds are achieved by reactions with piperidine,¹¹ phenanthroline, or diphenylacetylene¹² ligands. Treatment of **1a-c** with dpppe in refluxing acetonitrile yields mixtures of complexes $[\text{Mo}(\eta^3\text{-C}_3\text{H}_5)(\text{CO})\{\eta^2\text{-L}_2\}(\eta^2\text{-dpppe})]$ ($\text{L}_2 = \text{S}_2\text{CNC}_4\text{H}_8$, *endo*-, *exo*-**2**; S_2CNET_2 , *endo*-, *exo*-**3**; $\text{S}_2\text{P}(\text{OEt})_2$, *endo*-**4**) with *endo*:*exo* ratios of 6:1, 5:1, and 1:0, respectively (Scheme 1). The orientations of *endo* and *exo* are defined by the open face of the allyl group and carbonyl group being in the same direction in the former and opposite directions in the latter. These air-stable and orange-yellow compounds are obtained in high yields, which are easily soluble in chlorinated solvents but rather insoluble in nonpolar solvents. No appreciable decomposition of products was observed even upon prolonged standing of the precipitates in air.

From the discussion above, it is clear that the ratios of *endo* complexes are greater than those of *exo* complexes. To investigate the relation between orientations and phosphine ligand, we carried out the reactions of **1a-c** with dppm and dppa, respectively. The respective reactions of **1a-c** with dppm or dppa in an analogous manner result in isolation of the mixtures of complexes $[\text{Mo}(\eta^3\text{-C}_3\text{H}_5)(\text{CO})(\eta^2\text{-L}_2)(\eta^2\text{-dppm})]$ ($\text{L}_2 = \text{S}_2\text{CNC}_4\text{H}_8$,

(12) Yih, K. H.; Lee, G. H.; Huang, S. L.; Wang, Y. J. *Organomet. Chem.* **2002**, *658*, 191.

(13) (a) Graham, A. J.; Fenn, R. H. *J. Organomet. Chem.* **1969**, *17*, 405. (b) Brisdon, B. J.; Edwards, D. A.; Paddick, K. E.; Drew, M. G. B. *J. Chem. Soc., Dalton Trans.* **1980**, 1317.

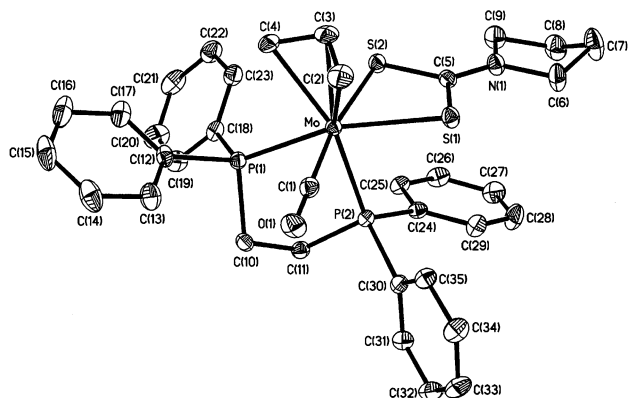


Figure 1. An ORTEP drawing with 50% thermal ellipsoids and atom-numbering scheme for the complex *endo*-[Mo(η^3 -C₃H₅)(η^2 -S₂CNC₄H₈)(CO)(η^2 -dppe)] (**2**).

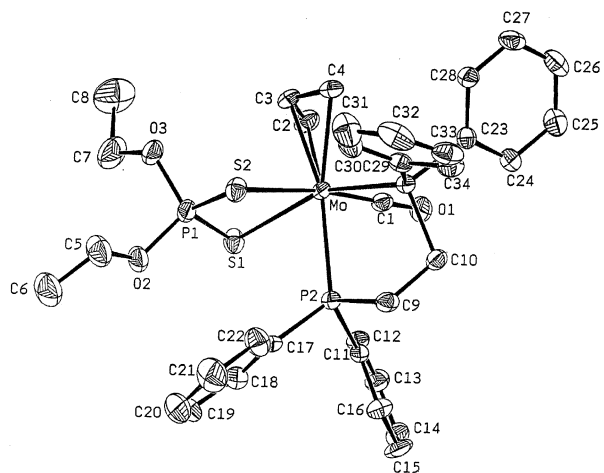


Figure 2. An ORTEP drawing with 30% thermal ellipsoids and atom-numbering scheme for the complex *endo*-[Mo(η^3 -C₃H₅){ η^2 -S₂P(OEt)₂}(CO)(η^2 -dppe)] (**4**).

endo-, *exo*-**5**; S₂CNET₂, *endo*-, *exo*-**6**; S₂P(OEt)₂, *endo*-, *exo*-**7**) with *endo*:*exo* ratios of 1:4, 1:9, and 2:1 or [Mo(η^3 -C₃H₅)(CO)(η^2 -L₂)(η^2 -dppa)] (L₂ = S₂CNC₄H₈, *endo*-, *exo*-**8**; S₂CNET₂, *endo*-, *exo*-**9**; S₂P(OEt)₂, *endo*-**10**) with *endo*:*exo* ratios of 1:1, 1:1, and 1:0 (Scheme 1). The air-stable yellow-orange compounds **5–10** are soluble in dichloromethane, slightly soluble in acetonitrile, and insoluble in diethyl ether and *n*-hexane. The isolated compounds **2–10** were already of good purity, but analytically pure samples could be obtained by slow *n*-hexane diffusion into a dichloromethane solution at +4 °C. All characterization data are consistent with the proposed constitution.

X-ray Single-Crystal Structures of *endo*-2, *endo*-4, *endo*-, *exo*-5, and *endo*-7. For satisfactory structural characterization, we performed X-ray diffraction studies of *endo*-**2**, *endo*-**4**, *endo*-, *exo*-**5**, and *endo*-**7** to elucidate the *endo* and *exo* conformers at 150 (**2**, **5**) and 298 K (**4**, **7**). ORTEP plots of the four complexes are shown in Figures 1–4. Table 2 contains selected bond distances and angles of the four complexes. Clearly, the open face of the allyl group is oriented toward the carbonyl group in *endo*-**2**, **-4**, **-5**, and **-7** and in the opposite direction in *exo*-**5**. In the four structures, the coordination geometry around the molybdenum atom is approximately an octahedron with the two sulfur atoms of the dithio ligand, two phosphorus atoms of the diphos ligand,

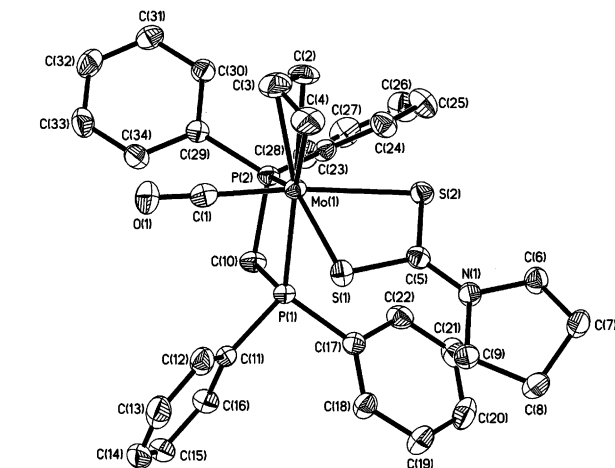
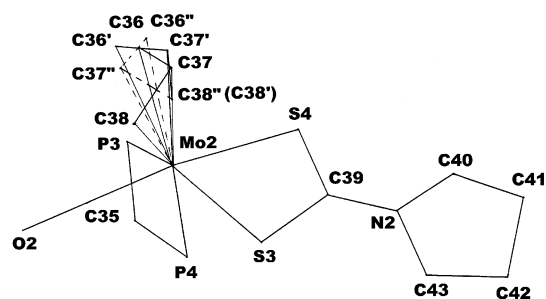


Figure 3. Disorder drawing of *endo*-[Mo(η^3 -C₃H₅)(η^2 -S₂CNC₄H₈)(CO)(η^2 -dppm)] (**5**) and an ORTEP drawing with 30% thermal ellipsoids and atom-numbering scheme for the complex *exo*-[Mo(η^3 -C₃H₅)(η^2 -S₂CNC₄H₈)(CO)(η^2 -dppm)] (**5**).

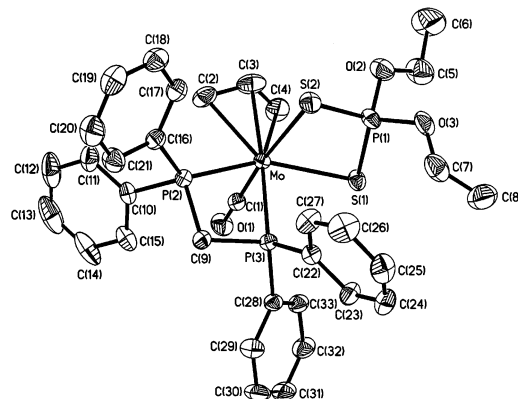


Figure 4. An ORTEP drawing with 30% thermal ellipsoids and atom-numbering scheme for the complex *endo*-[Mo(η^3 -C₃H₅){ η^2 -S₂P(OEt)₂}(CO)(η^2 -dppm)] (**7**).

carbonyl, and the allyl group occupying the six coordination sites. The four structures confirm unequivocal allyl groups. One of the sulfur atoms of the dithio ligand is *trans* to the diphos, S(1)–Mo–P(1), 141.421(19)–157.10(6)°, while the other is *trans* to carbonyl, S(2)–Mo–C(4), 170.48(7)–174.23(15)°. The S(1)–Mo–S(2) angles 68.071(17)–68.459(17)° in dithiocarbamate complexes are smaller than 75.27(57)–76.02(5)° in dithiophosphate complexes because of the different PS₂ and CS₂ hybridization of the P and C atoms. An examination of the S(1)–C(5)–S(2) bond distances and angles shows a geometrical environment characteristic of a sp² hybridization of the carbon atom. In addition, the S(1)–C(5)–S(2) angles in the range of 114.90(12)–115.96(12)°

Table 1. Crystal Data and Refinement Details for Complexes
endo-[Mo(η^3 -C₃H₅)(η^2 -S₂CNC₄H₈)(CO)(η^2 -dpppe)] (2)·CH₂Cl₂, *endo*-[Mo(η^3 -C₃H₅){ η^2 -S₂P(OEt)₂}(CO)(η^2 -dpppe)] (4)
endo- and *exo*-[Mo(η^3 -C₃H₅)(η^2 -S₂CNC₄H₈)(CO)(η^2 -dppm)] (5)·¹/₂CH₂Cl₂, and
endo-[Mo(η^3 -C₃H₅){ η^2 -S₂P(OEt)₂}(CO)(η^2 -dppm)] (7)

	2·CH ₂ Cl ₂	4	5· ¹ / ₂ CH ₂ Cl ₂	7
mol formula	C ₃₆ H ₃₉ Cl ₂ NOP ₂ S ₂ Mo	C ₃₄ H ₃₉ O ₃ P ₃ S ₂ Mo	C _{68.5} H ₇₁ ClN ₂ O ₂ P ₄ S ₄ Mo ₂	C ₃₃ H ₃₇ O ₃ P ₃ S ₂ Mo
fw	794.58	748.66	1433.72	734.61
cryst syst	monoclinic	monoclinic	triclinic	triclinic
cryst dimens, mm ³	0.40 × 0.40 × 0.25	0.25 × 0.30 × 0.35	0.30 × 0.25 × 0.35	0.20 × 0.35 × 0.40
space group	<i>P</i> 2 ₁ / <i>n</i>	<i>P</i> 2 ₁ / <i>c</i>	<i>P</i> 1	<i>P</i> 1
<i>a</i> , Å	11.3200(1)	9.915(2)	13.1526(1)	8.651(8)
<i>b</i> , Å	15.8152(2)	12.236(1)	15.8505(1)	14.090(3)
<i>c</i> , Å	19.6732(2)	28.591(5)	17.4172(1)	15.045(7)
α , deg			116.0641(3)	81.74(3)
β , deg	90.3932(4)	95.05(1)	92.4616(3)	78.43(7)
γ , deg			99.2887(3)	72.21(6)
<i>V</i> , Å ³	3521.97(7)	3455.1(10)	3192.35(4)	1703.8(17)
<i>Z</i>	4	4	2	2
<i>d</i> _{calcd} , g cm ⁻³	1.499	1.439	1.492	1.369
μ (Mo K α), mm ⁻¹	0.764	0.6541	0.713	0.6624
θ range, deg	1.65–27.50	18.96–24.18(2 θ)	1.31–27.50	0–45
<i>T</i> , °C	–123	25	–123	25
total no. of rflns	8065	4500	14649	4386
no. of parameters	407	389	799	379
<i>R</i> ^b	0.029	0.037	0.030	0.035
<i>Rw</i> ^c	0.074	0.032	0.075	0.030
<i>S</i> ^d	1.118	1.81	1.090	1.90

^a **5** contains two independent molecules in the unit cell. ^b $R = \sum ||F_o| - |F_c|| / \sum |F_o|$. ^c $Rw = [\sum w(|F_o| - |F_c|)^2]^{1/2}$; $w = 1/\sigma^2(|F_o|)$. ^d Quality-of-fit = $[\sum w(|F_o| - |F_c|)^2 / (N_{\text{obsd}} - N_{\text{parameters}})]^{1/2}$.

are significantly different from the S(1)–P–S(2) angles which are in the range of 109.67(10)–111.07(10)°.

The short C(5)–N bond length 1.322(3)–1.324(3) Å of the dithiocarbamate complexes **2** and **5** indicates a considerable partial double bond character (C–N = 1.47 Å, C=N = 1.225 Å, C≡N = 1.16 Å). The Mo–S(1) distance (trans to phosphorus) is clearly shorter than Mo–S(2) (trans to CO) because of the greater trans effect induced by the CO group than the phosphine group. Similarly, the Mo–P(1) distance (trans to sulfur) is slightly shorter than Mo–P(2) (trans to allyl) because of the greater trans effect induced by the allyl group than the dithiocarbamate group. The Mo–S (2.5467(6)–2.709(3) Å) and Mo–allyl (2.242(6)–2.406(6) Å) bond distances are consistent with the values reported for Mo^{II}–S and numerous Mo–allyl systems.^{5,13} The bond distances and intercarbon angle of allyl group in complexes **2**, **4**, **5**, and **7** (1.303(10)–1.399(3) Å, 1.363(10)–1.423(3) Å, and 116.8(2)–126.4(7)°) are insignificantly different and close to the region of related Mo^{II}–allylic compounds (1.31–1.42 Å, 115–125°).^{5,13} The Mo–P bond lengths are in the region of 2.4188(16)–2.5562(16) Å, and appear to be normal. The carbonyl ligand is essentially linear with a region of 176.83(19)–179.0(5)°. The values for the Mo–CO angles are similar to those found for other terminal carbonyls contained in Mo systems. The Mo–CO (1.895(6)–1.925(2) Å) and C–O distances are both within the range of values reported for other molybdenum carbonyl complexes.^{5,7,9,12,13}

X-ray structure determination of **5** at 150 K reveals the presence of two crystallographically inequivalent molecules in the unit cell, which differ mainly by the orientation of the allyl group with respect to the carbonyl group. The two molecules *endo*-**5** and *exo*-**5** with a ratio of 0.379:0.621 were depicted in Figure 3 together with the labeling scheme. The *endo*-**5** contains three disorder allyl groups, two *endo* orientations (C36, C37, C38 and C36', C37', C38'), and one *exo* orientation

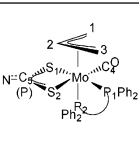
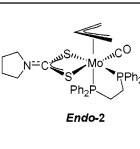
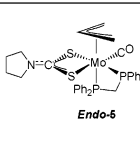
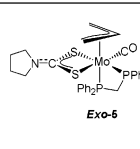
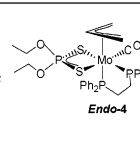
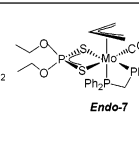
(C36'', C37'', C38'', see Figure 4). The site occupancy ratio is 0.195:0.093:0.092 and C38' and C38'' disorder at the same position. The total ratio of *endo*-**5**:*exo*-**5** is 0.288:0.712 in the solid state and 1:4 in the solution state by integration from ³¹P{¹H} NMR spectra. The crystal structure of **5** clearly shows that the *exo* form is favored in both solid and solution state. To our knowledge, the concomitant presence of two different allyl rotational isomers of this kind in one unit cell has been rarely noted.¹⁴

IR and MS Spectroscopy. The presence of a carbonyl group for all complexes in this work is clearly reflected in the IR spectra. In KBr, only one terminal carbonyl-stretching band is found, although both isomers are known to be present in different ratios. Because of limited solubility all IR spectra needed to be recorded in CH₂Cl₂, and therefore any small difference might be obscured by the natural line-broadening in this solvent. In the FAB mass spectra, base peaks with the typical Mo isotope distribution are in agreement with the [M⁺] for complexes **2**, **5**, **8**, **9**, and **10** and [M⁺ – CO] for complexes **3**, **4**, **6**, and **7**.

NMR Spectroscopy. The ¹H and ¹³C{¹H} NMR spectral data for the series of [Mo(η^3 -C₃H₅)(η^2 -dithio)(CO)(η^2 -diphos)] complexes **2**–**9** are obtained only for the major products, because of the low ratio and no isolation of the minor products (see Experimental Section). Interestingly, their room temperature ¹H NMR spectra exhibit five sets of resonances for the allyl moiety typical of the ABCDX spin patterns of unsymmetrical η^3 -allyl dithiocarbamate metal complexes and of the AA'BB'X spin patterns of symmetrical η^3 -allyl dithiophosphate metal complexes. In the ¹H NMR spectrum of *exo*-**5**, the methylene protons of the dppm ligand and allyl protons exhibit seven equally intense

(14) (a) Gorfti, A.; Salmain, M.; Jaouen, G.; McGlinchey, M.; Bennouna, A.; Mousser, A. *Organometallics* **1996**, *15*, 142. (b) van Staveren, D. R.; Weyhermuller, T.; Metzler-Nolte, N. *Organometallics* **2000**, *19*, 3730.

Table 2. Selected Bond Distances (Å) and Angles (deg) for **2**, **4**, **5**, and **7**

						
	Bond Distances (Å)					
C ₁ -C ₂	1.399(3)	1.380(4)	1.398(4)	1.369(9)	1.303(10)	
C ₂ -C ₃	1.423(3)	1.400(4)	1.377(4)	1.397(9)	1.363(10)	
Mo-C ₁	2.349(2)	2.417(4)	2.339(2)	2.354(6)	2.406(6)	
Mo-C ₂	2.230(2)	2.281(4)	2.325(2)	2.242(6)	2.300(6)	
Mo-C ₃	2.305(2)	2.290(5)	2.369(2)	2.309(6)	2.358(6)	
Mo-C ₄	1.925(2)	1.911(2)	1.916(2)	1.895(6)	1.908(6)	
Mo-P ₁	2.4425(6)	2.4217(5)	2.4336(5)	2.4368(16)	2.4188(16)	
Mo-P ₂	2.5225(5)	2.5012(5)	2.4439(5)	2.5562(16)	2.4975(22)	
Mo-S ₁	2.5588(5)	2.6250(5)	2.5467(6)	2.6095(17)	2.5806(16)	
Mo-S ₂	2.6248(5)	2.5147(6)	2.6181(6)	2.6756(17)	2.709(3)	
C ₅ (P)-S ₁	1.723(2)	1.722(2)	1.726(2)	1.9791(23)	1.994(3)	
C ₅ (P)-S ₂	1.720(2)	1.712(2)	1.709(2)	1.9689(23)	1.9591(22)	
N-C ₅	1.322(3)	1.324(3)	1.324(3)	-	-	
	Bond Angles (deg)					
C ₁ -C ₂ -C ₃	116.8(2)	118.1(5)	120.9(3)	116.9(6)	126.4(7)	
P ₁ -Mo-P ₂	78.858(18)	67.348(17)	67.890(17)	79.16(5)	67.73(6)	
S ₁ -Mo-S ₂	68.071(17)	68.958(17)	68.459(17)	76.02(5)	75.27(7)	
S ₁ -C ₅ (P)-S ₂	114.90(12)	115.96(12)	115.53(12)	111.07(10)	109.67(10)	
S ₁ -Mo-P ₁	156.160(19)	147.26(2)	141.421(19)	157.10(6)	147.35(6)	
S ₂ -Mo-C ₄	170.65(6)	171.01(6)	170.48(7)	172.42(17)	174.23(15)	
Mo-C ₄ -O	179.45(19)	176.83(19)	178.4(2)	179.0(5)	177.2(4)	

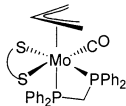
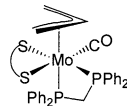
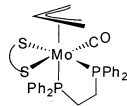
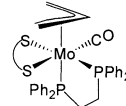
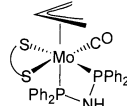
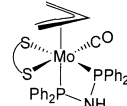
resonances at δ 3.97, 4.23 and at δ 2.48, 2.63 (H_{anti}), δ 2.35, 4.08 (H_{syn}), δ 4.95 (H_{center}), respectively. The corresponding $^{13}\text{C}\{^1\text{H}\}$ NMR signals are at δ 41.8 and δ 54.6, 71.7, 101.4. In the $^{13}\text{C}\{^1\text{H}\}$ NMR spectrum of *exo-5*, two resonances appear in the carbonyl region. The one resonance at δ 227.6 is attributed to the carbonyl group and the resonance at δ 204.0 is assigned to the carbon atom of the CS_2 of the $\text{C}_4\text{H}_8\text{NCS}_2$ ligand. The other ^1H and $^{13}\text{C}\{^1\text{H}\}$ NMR spectra of complexes **2–9** are similar to that of **5**.

The $^{31}\text{P}\{^1\text{H}\}$ NMR spectral data are summarized in Table 3. Compared to the $^{31}\text{P}\{^1\text{H}\}$ NMR spectra and the structures of the complexes *endo-2*, *endo-4*, *exo-5*, and *endo-7*, it can be concluded that (1) the dithiophosphato ligand improves the formation of endo-products, whereas the dithiocarbamate ligands improve the formation of endo products in dppe ligand and exo products in dppm

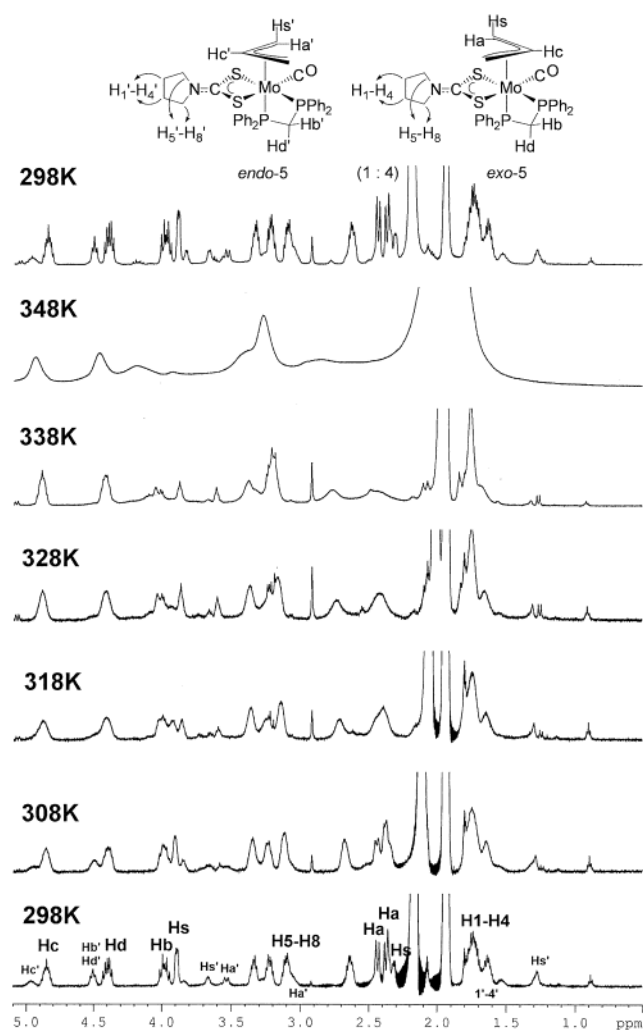
ligand, (2) *exo* complexes show larger $J_{\text{P-P}}$ coupling constants than those of *endo* complexes, and (3) the resonances of dppm and dppe complexes appear in relative up-field for the *exo* orientation and dppe complexes appear in the relative up-field for the *endo* orientation.

To investigate the interconversion of complexes *endo-3* and *endo-5*, the variable-temperature ^1H and $^{31}\text{P}\{^1\text{H}\}$ NMR experiments were undertaken in the range of 183–348 K. In the range of 183–298 K, the ratio was retained and only one H_{anti} proton resonance of the allyl ligand and one methylene proton resonance of dppm ligand shifted from 3.99 to 3.85 ppm and from 2.67 to 2.32 ppm of *exo-5*, respectively (Supporting Information, spectrum A). Addition of free diphos ligands dppm, dppe, or dithiocarbamate ligands $\text{Et}_2\text{NCS}_2^-$, $\text{C}_4\text{H}_8\text{NCS}_2^-$ had no effect on these variable-temperature

Table 3. $^{31}\text{P}\{^1\text{H}\}$ NMR Data for Endo and Exo Complexes

							
	<i>endo</i>	<i>exo</i>	<i>endo</i>	<i>exo</i>	<i>endo</i>	<i>exo</i>	
Ratio	1:4		6:1		1:1		
$\text{C}_4\text{H}_8\text{NCS}_2^-$	δ	4.7, 32.4	1.8, 26.9	54.5, 82.3	63.0, 85.8	59.9, 97.7	59.7, 91.6
	$J_{\text{P-P}}$	48.1	61.6	26.1	39.1	61.1	79.0
$\text{Et}_2\text{NCS}_2^-$	Ratio	1:9		5:1		1:1	
	δ	2.5, 31.2	-0.8, 26.2	53.3, 82.9	62.2, 86.6	58.9, 97.7	58.3, 91.6
	$J_{\text{P-P}}$	51.0	64.1	26.1	39.3	62.9	79.5
$(\text{EtO})_2\text{PS}_2^-$	Ratio	2:1		1:0		1:0	
	δ	-2.6, 33.4	-7.0, 30.8	45.9, 82.9		52.0, 97.6	
	$J_{\text{P-P}}$	49.5	67.8	26.6		61.1	

spectra of *endo*-, *exo*-**3** and **5** and therefore a rearrangement involving a π - σ - π^3 process or dissociation of the diphos or dithiocarbamate ligand seems unlikely. As depicted in Figure 5, the variable-temperature ^1H NMR spectra were undertaken in CD_3CN from 298 to 348 K. For **5**, 10 signals were observed at room temperature for the allyl ligand: five for the *endo* and five for the *exo* isomers. In contrast, five signals were observed for the allyl ligand at 318 K, due to rapid interconversion of *endo*-**5** to *exo*-**5** on the NMR time scale. However, board signals were observed at 348 K, due to rapid allyl rotation. Noticeably, the original ratios and the proton resonances of *endo*-**5** and *exo*-**5** were retained when the variable-temperature experiments were finished. The activation energies¹⁵ for the interconversion of *endo*-**5** to *exo*-**5** in CD_3CN were determined to be $\Delta G^\ddagger = 65.1 \pm 0.4 \text{ kJ mol}^{-1}$ at 318 K and $\Delta G^\ddagger = 61.5 \pm 0.4 \text{ kJ mol}^{-1}$ for *exo*-**3** to *endo*-**3** at 298 K in CDCl_3 (Supporting Information, spectrum B). The large activation energy of *endo*-, *exo*-**5** compared with *endo*- and *exo*-**3** is due to the bite angles and the fact that dppm increases the barrier most effectively. Compared with other intramolecular trigonal twist rearrangement complexes, the activation energy of *endo*-, *exo*-**3,5** are larger than those of complexes $[\text{M}(\eta^3\text{-C}_3\text{H}_5)(\text{CO})_2(\text{diphos})\text{I}]^{2c}$ ($\text{M} = \text{Mo}, \text{W}$; diphos = dppm, dppe) (41.8 – 49.8 kJ mol^{-1}) and $[\text{Mo}(\text{CO})(\eta^3\text{-allyl})\{\eta^2\text{-S}_2\text{P}(\text{OEt})_2\}(\text{X})]^{11}$ ($\text{X} = \text{CH}_3\text{CN}, 48.5 \text{ kJ mol}^{-1}$; $\text{C}_5\text{H}_{10}\text{NH}, 52.7 \text{ kJ mol}^{-1}$), and they are similar to the allyl rotation complex $[\text{Mo}(\eta^5\text{-C}_5\text{H}_4\text{-COPhe-OMe})(\eta^3\text{-allyl})(\text{CO})_2]$ (62.7 kJ mol^{-1}).^{14b} Rotation of the allyl group has been reported for complexes $[\text{CpMo}(\eta^3\text{-allyl})(\text{CO})_2]^1$ but for no example in the bidentate $\text{Mo}(\eta^3\text{-allyl})(\eta^2\text{-L})$ system. The spectral observations of the dynamic species and the data of activation energy⁶ of complexes *endo*-, *exo*-**3,5** reveal that the isomers undergo mutual exchange by rotation of the metal–allyl bond.

**Figure 5.** Variable-temperature ^1H NMR observations of the mixture *endo*-**5** and *exo*-**5** in CD_3CN .

Concluding Remarks

We employ three different diphos ligands to investigate the dependence of the ratio and interconversion of

(15) (a) Hesse, M.; Meier, H.; Zeeh, B. *Spektroskopische Methoden in der Organischen Chemie*, 3rd ed.; Georg Thieme Verlag: Stuttgart, New York, 1987. (b) Günther, H. *La Spectroscopie de RMN*; Masson: Paris, France, 1993.

the endo and exo conformer. The dithiophosphato ligand improves the formation of endo products, whereas the dithiocarbamate ligands improve the formation of endo products in the dppe ligand and of exo products in the dppm ligand. The exo complexes show larger J_{P-P} coupling constants than endo complexes. The resonances of dppm and dpa complexes appear in relative up-field positions for the exo orientation and dppe complexes appear in relative up-field positions for the endo orientation. To our knowledge, the X-ray crystal structure of *endo*-, *exo*-**5** is the first reported example to have different orientations of the allyl group with respect to the carbonyl group of a simple $M(\eta^3-C_3H_5)(\eta^2-L)(CO)$ complex. Furthermore, it is one of the rare examples in which two isomers that differ primarily by rotation about the metal–allyl axis are present in the unit cell. In addition, the allyl endo \leftrightarrow exo interconversion activation barriers of **5** and **3** are determined. The large activation energy of *endo*-, *exo*-**5** compared with *endo*-, *exo*-**3** is due to the bite angles and the fact that dppm increases the barrier most effectively.

Experimental Section

General Procedures. All manipulations were performed under nitrogen using vacuum-line, drybox, and standard Schlenk techniques. NMR spectra were recorded on a Bruker AM-200 or on an AM-500 WB FT-NMR spectrometer and are reported in units of parts per million with residual protons in the solvent as an internal standard ($CDCl_3$, δ 7.24; CD_3CN , δ 1.93; C_2D_6CO , δ 2.04). IR spectra were measured on a Nicolet Avator-320 instrument and referenced to polystyrene standard, using cells equipped with calcium fluoride windows. MS spectra were recorded on a JEOL SX-102A spectrometer. Solvents were dried and deoxygenated by refluxing over the appropriate reagents before use. *n*-Hexane, diethyl ether, THF, and benzene were distilled from sodium-benzophenone. Acetonitrile and dichloromethane were distilled from calcium hydride, and methanol was distilled from magnesium. All other solvents and reagents were of reagent grade and used as received. The compounds $[Mo(\eta^3-C_3H_5)(CO)_2(\eta^2-S_2CNC_4H_8)]$ (**1a**),¹⁰ $[Mo(\eta^3-C_3H_5)(CO)_2(\eta^2-S_2CNET_2)]$ (**1b**), and $[Mo(CH_3CN)(\eta^3-C_3H_5)(CO)_2\{\eta^2-S_2P(OEt)_2\}]$ (**1c**)¹¹ were prepared according to the literature methods. The ΔG^\ddagger values were calculated with the Eyring equation^{15b} $\Delta G^\ddagger = RT_c(22.96 + \ln T/\Delta\nu)$ [$J \cdot mol^{-1}$] where T_c (K) is the temperature of coalescence of two given signals and $\Delta\nu$ (Hz) is the difference in their chemical shifts at exchange temperature; the error is estimated to be ± 0.4 $kJ \cdot mol^{-1}$. Elemental analyses and X-ray diffraction studies were carried out at the Regional Center of Analytical Instrument located at the National Taiwan University. $Mo(CO)_6$ and C_3H_5Br were purchased from Strem Chemical, $C_4H_8NCS_2NH_4$, Et_2NCS_2Na , $(EtO)_2PS_2NH_4$, dppm, dppe, and dpa were purchased from Merck.

Preparation of 2. MeCN (20 mL) was added to a flask (100 mL) containing a mixture of dppe (0.398 g, 1.0 mmol) and $[Mo(\eta^3-C_3H_5)(CO)_2(\eta^2-S_2CNC_4H_8)]$ (0.339 g, 1.0 mmol). The solution was refluxed for 1 h, and an IR spectrum indicated completion of the reaction. After removal of the solvent in vacuo, the residue was redissolved with CH_2Cl_2 (10 mL). *n*-Hexane (25 mL) was added to the solution and yellow-orange solids of **2** were formed which were isolated by filtration (G4), washed with *n*-hexane (2×10 mL), and subsequently dried under vacuum yielding a mixture of *endo*-, *exo*- $[Mo(\eta^3-C_3H_5)(\eta^2-S_2CNC_4H_8)(CO)(\eta^2-dppe)]$ (**2**) (0.57 g, 80%) as a yellow-orange microcrystalline solid. Further purification was accomplished by recrystallization from 1/10 CH_2Cl_2/n -hexane. Spectroscopic data of **2** are as follows. IR (KBr, cm^{-1}): $\nu(CO)$ 1791 (vs). MS (FAB, NBA, m/z): 711 (M^+), 683 ($M^+ - CO$), 642 ($M^+ - CO - C_3H_5$). Anal. Calcd. for $C_{35}H_{37}NOP_2S_2Mo$: C, 59.23; H, 5.26;

N, 1.97. Found: C, 59.42; H, 5.38; N, 1.85. $^{31}P\{^1H\}$ NMR (202 MHz, $CDCl_3$, 298 K): *endo*-**2** δ 54.5, 82.3 (d, $^2J_{P-P} = 20.8$ Hz); *exo*-**2** δ 63.0, 85.8 (br). $^{31}P\{^1H\}$ NMR (202 MHz, $CDCl_3$, 278 K): *endo*-**2** δ 54.5, 82.3 (d, $^2J_{P-P} = 26.1$ Hz); *exo*-**2** δ 62.8, 86.0 (d, $^2J_{P-P} = 39.1$ Hz). *endo*-**2**: 1H NMR (500 MHz, $CDCl_3$, 298 K): δ 1.57, 1.67 (m, 2H, NCH_2CH_2), 2.11 (m, 1H, H_{syn}), 2.43 (d, 2H, H_{anti} , $J_{H-H} = 10.6$ Hz), 2.25, 2.74, 2.95, 3.27 (m, 4H, NCH_2), 2.81, 4.08 (m, 4H, PCH_2), 3.14 (m, 2H, H_{syn}) 4.35 (m, 1H, H_c), 6.91–8.16 (m, 20H, Ph). $^{13}C\{^1H\}$ NMR (125 MHz, $CDCl_3$, 298 K): δ 24.3, 24.5 (s, NCH_2CH_2), 25.5 (t, PCH_2 , $J_{P-C} = 18.4$ Hz), 48.5, 48.9 (s, NCH_2), 71.6, 87.3 (s, $=CH_2$), 116.4 (s, $=CH$), 127–134 (m, Ph), 206.2 (s, NCS_2), 229.1 (t, CO, $^2J_{P-C} = 16.1$ Hz).

Preparation of 3. The synthesis and workup were similar to those used in the preparation of complex **2**. The complex *endo*-, *exo*- $[Mo(\eta^3-C_3H_5)(\eta^2-S_2CNET_2)(CO)(\eta^2-dppe)]$ (**3**) was isolated in 85% yield as a yellow-orange microcrystalline solid. Spectroscopic data of **3** are as follows. IR (KBr, cm^{-1}): $\nu(CO)$ 1781 (vs). $^{31}P\{^1H\}$ NMR (202 MHz, $CDCl_3$, 298K): *exo*-**3** δ 62.0, 86.4 (br), *endo*-**3** δ 53.4, 82.7 (br). $^{31}P\{^1H\}$ NMR (202 MHz, $CDCl_3$, 278 K): *exo*-**3** δ 62.3, 86.6 (d, $^2J_{P-P} = 39.3$ Hz), *endo*-**3** δ 53.3, 82.9 (d, $^2J_{P-P} = 26.1$ Hz). MS (FAB, NBA, m/z): 685 ($M^+ - CO$), 644 ($M^+ - CO - C_3H_5$). Anal. Calcd for $C_{35}H_{39}NOP_2S_2Mo$: C, 59.06; H, 5.52; N, 1.97. Found: C, 59.25; H, 5.75; N, 1.82. *endo*-**3**: $^{13}C\{^1H\}$ NMR (125 MHz, $CDCl_3$, 298 K): δ 12.1, 12.3 (s, NCH_2CH_3), 32.3 (t, PCH_2 , $J_{P-C} = 18.4$ Hz), 43.8, 44.4 (s, NCH_2), 57.2, 83.7 (s, $=CH_2$), 115.2 (s, $=CH$), 126.1–137.7 (m, Ph), 208.2 (s, NCS_2), 229.3 (s, CO).

Preparation of 4. The synthesis and workup were similar to those used in the preparation of complex **2**. The complex *endo*- $[Mo(\eta^3-C_3H_5)\{\eta^2-S_2P(OEt)_2\}(CO)(\eta^2-dppe)]$ (**4**) was isolated in 87% yield as a yellow-orange microcrystalline solid. Spectroscopic data of *endo*-**4** are as follows. IR (KBr, cm^{-1}): $\nu(CO)$ 1801 (vs). $^{31}P\{^1H\}$ NMR (81 MHz, $CDCl_3$, 298 K): δ 45.9 (d, $J_{P-P} = 26.6$ Hz, dppe), 82.9 (d, $J_{P-P} = 26.6$ Hz, dppe), 96.4 (PS_2). 1H NMR (200 MHz, $CDCl_3$, 298 K): δ 0.40 (m, 2H, H_{anti}), 0.79, 1.32 (t, 6H, OCH_2CH_3 , $J_{H-H} = 7.2$ Hz), 2.22 (m, 2H, PCH_2), 2.58 (d, 2H, H_{syn} , $J_{H-H} = 10.8$ Hz), 2.84 (m, 2H, OCH_2), 3.10 (m, 2H, PCH_2), 4.02 (m, 2H, OCH_2), 4.58 (m, 1H, H_c). $^{13}C\{^1H\}$ NMR (50 MHz, $CDCl_3$, 298 K): δ 15.5, 15.9 (d, OCH_2CH_3 , $^3J_{P-C} = 8.4$ Hz), 31.6 (t, PCH_2 , $J_{P-C} = 10.4$ Hz), 60.6, 61.4 (d, OCH_2 , $^2J_{P-C} = 10.0$ Hz), 74.6, 86.4 (s, $=CH_2$), 114.8 (br, $=CH$), 126.7–137.8 (m, Ph), 228.6 (s, CO). MS (FAB, NBA, m/z) 721.5 ($M^+ - CO$). Anal. Calcd for $C_{34}H_{39}O_3P_2S_2Mo$: C, 54.54; H, 5.26. Found: C, 54.76; H, 5.40.

Preparation of 5. The synthesis and workup were similar to those used in the preparation of complex **2**. The complex *endo*-, *exo*- $[Mo(\eta^3-C_3H_5)(\eta^2-S_2CNC_4H_8)(CO)(\eta^2-dppm)]$ (**5**) was isolated in 82% yield as a yellow-orange microcrystalline solid. Spectroscopic data of **5** are as follows. IR (KBr, cm^{-1}): $\nu(CO)$ 1781 (vs). MS (FAB, NBA, m/z): 697 (M^+), 669 ($M^+ - CO$), 628 ($M^+ - CO - C_3H_5$). Anal. Calcd for $C_{34}H_{35}NOP_2S_2Mo$: C, 58.70; H, 5.07; N, 2.01. Found: C, 58.76; H, 5.32; N, 1.94. $^{31}P\{^1H\}$ NMR (202 MHz, $CDCl_3$, 298K): *endo*-**5** δ 4.7, 32.4 (d, $^2J_{P-P} = 48.1$ Hz); *exo*-**5** δ 1.8, 26.9 (d, $^2J_{P-P} = 61.6$ Hz). *endo*-**5**: 1H NMR (500 MHz, $CDCl_3$, 298 K): δ 1.36, 2.75 (br, 2H, H_{syn}), 1.60, 1.78 (m, 4H, NCH_2CH_2), 3.73 (d, 2H, H_{anti} , $J_{H-H} = 12.7$ Hz), 3.04–3.38 (m, 4H, NCH_2), 4.40, 4.47 (m, 2H, PCH_2), 5.13 (m, 1H, H_c), 6.92–7.84 (m, 20H, Ph). *exo*-**5**: 1H NMR (500 MHz, $CDCl_3$, 298 K): δ 1.66, 1.72 (m, 2H, NCH_2CH_2), 2.35 (m, 1H, H_{syn} , $J_{P-H} = 3.8$ Hz), 2.48, 2.63 (d, 2H, H_{anti} , $J_{H-H} = 10.9$, 11.7 Hz), 2.69, 3.11, 3.19, 3.40 (m, 4H, NCH_2), 3.97 (dt, 1H, PCH_2 , $J_{H-H} = 15.1$ $J_{P-H} = 9.7$ Hz), 4.08 (m, 1H, H_{syn} , $J_{H-H} = 7.1$ $J_{P-H} = 2.7$ Hz), 4.23 (dt, 1H, PCH_2 , $J_{H-H} = 15.1$ Hz, $J_{P-H} = 8.4$ Hz), 4.95 (m, 1H, H_c), 6.92–7.84 (m, 20H, Ph). $^{13}C\{^1H\}$ NMR (100 MHz, $CDCl_3$, 298 K): δ 24.7, 25.1 (s, NCH_2CH_2), 41.8 (t, PCH_2 , $J_{P-C} = 19.3$ Hz), 49.1, 49.6 (s, NCH_2), 54.6, 71.7 (d, $=CH_2$, $^2J_{P-C} = 13.9$, 9.0 Hz), 101.4 (s, $=CH$), 127–134 (m, Ph), 204.0 (d, CS_2 , $^3J_{P-C} = 3.6$ Hz), 227.6 (s, CO).

Preparation of 6. The synthesis and workup were similar to those used in the preparation of complex **2**. The complex

endo-,*exo*-[Mo(η^3 -C₃H₅)(η^2 -S₂CNEt₂)(CO)(η^2 -dppm)] (**6**) was isolated in 87% yield as a yellow-orange microcrystalline solid. Spectroscopic data of **6** are as follows. IR (KBr, cm⁻¹): ν (CO) 1806 (vs). MS (FAB, NBA, *m/z*): 671 (M⁺ - CO). ³¹P{¹H} NMR (202 MHz, CDCl₃, 298 K): *endo*-**6** δ 2.5, 31.2 (d, ²J_{P-P} = 51.0 Hz); *exo*-**6** δ -0.8, 26.2 (d, ²J_{P-P} = 64.1 Hz). Anal. Calcd for C₃₃H₃₇NOP₂S₂Mo: C, 58.53; H, 5.35; N, 2.01. Found: C, 58.76; H, 5.40; N, 1.98. *exo*-**6**: ¹H NMR (200 MHz, CDCl₃, 298 K): δ 0.74, 1.02 (t, 6H, NCH₂CH₃, J_{H-H} = 7.1 Hz), 2.32, 2.43 (m, 1H, H_{syn}, J_{H-H} = 6.4, J_{P-H} = 3.6 Hz), 2.45, 2.50 (d, 2H, H_{anti}, J_{H-H} = 9.8 Hz), 3.23, 3.45 (m, 4H, NCH₂), 3.92, 4.05 (m, 2H, PCH₂), 4.00 (m, 1H, H_{syn}), 4.86 (m, 1H, H_c), 6.89–7.81 (m, 20H, Ph). ¹³C{¹H} NMR (50 MHz, CDCl₃, 298 K): δ 12.6 (s, NCH₂CH₂), 42.3 (t, PCH₂, J_{P-C} = 20.2 Hz), 44.1, 44.8 (s, NCH₂), 55.0, 72.4 (s, =CH₂), 101.2 (s, =CH), 127.1–137.2 (m, Ph), 208.2 (s, CS₂), 228.2 (s, CO).

Preparation of 7. The synthesis and workup were similar to those used in the preparation of complex **2**. The complex *endo*-, *exo*-[Mo(η^3 -C₃H₅){ η^2 -S₂P(OEt)₂}(CO)(η^2 -dppm)] (**7**) was isolated in 82% yield as a yellow-orange microcrystalline solid. Spectroscopic data of **7** are as follows. IR (KBr, cm⁻¹): ν (CO) 1799 (vs). MS (FAB, NBA, *m/z*): 708 (M⁺ - CO). Anal. Calcd for C₃₃H₃₇O₃P₃S₂Mo: C, 53.95; H, 5.09. Found: C, 54.12; H, 5.53. ³¹P{¹H} NMR (202 MHz, CDCl₃, 298 K): *exo*-**7**: δ -7.0, 30.8 (d, ²J_{P-P} = 67.8 Hz), 102.1; *endo*-**7** δ -2.6, 33.4 (d, ²J_{P-P} = 49.5 Hz), 97.5. ¹H NMR (200 MHz, CDCl₃, 298 K): δ 0.72, 1.27 (t, 6H, OCH₂CH₃, J_{H-H} = 7.1 Hz), 2.62, 2.95 (m, 4H, OCH₂), 2.82 (m, 2H, H_{anti}), 3.62, 3.91 (m, 2H, H_{syn}), 3.92, 4.58 (m, 2H, PCH₂), 4.92 (m, 1H, H_c), 6.70–7.85 (m, 20H, Ph). ¹³C{¹H} NMR (50 MHz, CDCl₃, 298 K): δ 15.1 (br, OCH₂CH₃), 45.3 (t, PCH₂, J_{P-C} = 10.4 Hz), 61.3 (br, OCH₂), 68.3, 81.3 (s, =CH₂), 100.9 (br, =CH), 127.2–134.8 (m, Ph), 209.1 (s, CO).

Preparation of 8. The synthesis and workup were similar to those used in the preparation of complex **2**. The complex *endo*-, *exo*-[Mo(η^3 -C₃H₅)(η^2 -S₂CNC₄H₈)(CO)(η^2 -dppa)] (**8**) was isolated in 88% yield as a yellow-orange microcrystalline solid. Spectroscopic data of **8** are as follows. Anal. Calcd for C₃₃H₃₄N₂OP₂S₂Mo: C, 56.89; H, 4.92; N, 4.02. Found: C, 56.76; H, 5.10; N, 4.04. IR (KBr, cm⁻¹): ν (CO) 1797 (vs). MS (FAB, NBA, *m/z*): 698 (M⁺), 670 (M⁺ - CO), 629 (M⁺ - CO - C₃H₅). ¹H NMR (500 MHz, CDCl₃, 298 K): δ 1.67, 1.71 (m, 2H, NCH₂CH₂), 2.67 (m, 1H, H_{syn}), 3.00, 3.54 (d, 2H, H_{anti}, J_{H-H} = 11.3, 11.4 Hz), 2.46, 3.86, 3.97, 4.45 (m, 4H, NCH₂), 4.14 (m, 1H, H_{syn}), 5.13 (m, 1H, H_c), 7.00–8.04 (m, 20H, Ph). ¹³C{¹H} NMR (125 MHz, CDCl₃, 298 K): δ 24.9, 25.1 (s, NCH₂CH₂), 49.2, 49.6 (s, NCH₂), 55.6, 74.7 (s, =CH₂), 110.5 (s, =CH), 126.2–138.7 (m, Ph), 202.9 (d, CS₂, ³J_{P-C} = 3.6 Hz), 228.7 (s, CO). ³¹P{¹H} NMR (202 MHz, CDCl₃, 298 K): *endo*-**8** δ 59.9, 97.7 (d, ²J_{P-P} = 61.1 Hz); *exo*-**8** δ 59.7, 91.6 (d, ²J_{P-P} = 79.0 Hz).

Preparation of 9. The synthesis and workup were similar to those used in the preparation of complex **2**. The complex *endo*-, *exo*-[Mo(η^3 -C₃H₅)(η^2 -S₂CNEt₂)(CO)(η^2 -dppa)] (**9**) was isolated in 84% yield as a yellow-orange microcrystalline solid. Spectroscopic data of **9** are as follows. Anal. Calcd for C₃₃H₃₆N₂OP₂S₂Mo: C, 56.73; H, 5.19; N, 4.01. Found: C, 56.56; H, 5.10; N, 3.94. IR (KBr, cm⁻¹): ν (CO) 1812 (vs). MS (FAB, NBA, *m/z*): 700 (M⁺), 672 (M⁺ - CO), 631 (M⁺ - CO - C₃H₅). ¹H NMR (500 MHz, CDCl₃, 298K): δ 0.72, 0.98 (br, 6H, NCH₂CH₃), 2.65, 4.09 (br, 2H, H_{syn}), 2.88, 3.55 (d, 2H, H_{anti}, J_{H-H} = 9.0 Hz), 2.25, 3.22, 3.90, 4.43 (m, 4H, NCH₂), 5.05 (m, 1H, H_c), 6.78–8.02 (m, 20H, Ph). ¹³C{¹H} NMR (125 MHz, CDCl₃, 298 K): δ 12.5 (s, NCH₂CH₃), 47.2 (s, NCH₂), 63.8, 74.8 (s, =CH₂), 115.0 (s, =CH), 127.9–137.3 (m, Ph), 202.8 (s, CS₂), 229.2 (s, CO). ³¹P{¹H} NMR (202 MHz, CDCl₃, 298 K): *endo*-**9** δ 58.9, 97.6 (d, ²J_{P-P} = 62.9 Hz); *exo*-**9** δ 58.3, 91.6 (d, ²J_{P-P} = 79.5 Hz).

Preparation of 10. The synthesis and workup were similar to those used in the preparation of complex **2**. The complex *endo*-[Mo(η^3 -C₃H₅){ η^2 -S₂P(OEt)₂}(CO)(η^2 -dppa)] (**10**) was isolated in 80% yield as a yellow-orange microcrystalline solid. Spectroscopic data of *endo*-**10** are as follows. Anal. Calcd for

C₃₂H₃₆NO₃P₃S₂Mo: C, 52.25; H, 4.93; N, 1.90. Found: C, 52.56; H, 5.10; N, 1.74. IR (KBr, cm⁻¹): ν (CO) 1806 (vs). MS (FAB, NBA, *m/z*): 737 (M⁺), 709 (M⁺ - CO), 668 (M⁺ - CO - C₃H₅). ³¹P{¹H} NMR (202 MHz, CDCl₃, 298 K): δ 52.0, 97.6 (d, ²J_{P-P} = 61.1 Hz), 96.7 (s, PS₂).

Single-Crystal X-ray Diffraction Analyses of 2, 4, 5, and 7. Single crystals of **2**, **4**, **5**, and **7** suitable from X-ray diffraction analyses were grown by recrystallization from 20:1 *n*-hexane/CH₂Cl₂. The diffraction data were collected at room temperature on an Enraf-Nonius CAD4 diffractometer equipped with graphite-monochromated Mo K α (λ = 0.71073 Å) radiation. The raw intensity data were converted to structure factor amplitudes and their esd's after correction for scan speed, background, Lorentz, and polarization effects. An empirical absorption correction, based on the azimuthal scan data, was applied to the data. Crystallographic computations were carried out on a Microvax III computer using the NRCC-SDP-VAX structure determination package.¹⁶

A suitable single crystal of **2** was mounted on the top of a glass fiber with glue. Initial lattice parameters were determined from 24 accurately centered reflections with θ values in the range from 1.65 to 27.50°. Cell constants and other pertinent data were collected and are recorded in Table 1. Reflection data were collected using the $\theta/2\theta$ scan method. The final scan speed for each reflection was determined from the net intensity gathered during an initial prescan and ranged from 2.06 to 8.24° min⁻¹. The θ scan angle was determined for each reflection according to the equation $0.80 \pm 0.35 \tan \theta$. Three check reflections were measured every 30 min throughout the data collection and showed no apparent decay. The merging of equivalent and duplicate reflections gave a total of 28690 unique measured data in which 8065 reflections with $I > 2\sigma(I)$ were considered observed. The structure was first solved by using the heavy-atom method (Patterson synthesis), which revealed the positions of metal atoms. The remaining atoms were found in a series of alternating difference Fourier maps and least-squares refinements. The quantity minimized by the least-squares program was $\omega(|F_o| - |F_c|)^2$, where ω is the weight of a given operation. The analytical forms of the scattering factor tables for the neutral atoms were used.¹⁷ The non-hydrogen atoms were refined anisotropically. Hydrogen atoms were included in the structure factor calculations in their expected positions on the basis of idealized bonding geometry but were not refined in least squares. All hydrogens were assigned isotropic thermal parameters 1–2 Å² larger than the equivalent B_{iso} value of the atom to which they were bonded. The final residuals of this refinement were $R = 0.029$ and $R_w = 0.074$. Selected bond distances and angles are listed in Table 2.

The procedures for **4**, **5**, and **7** were similar to those for **2**. The final residuals of this refinement were $R = 0.037$ and $R_w = 0.032$ for **4**, $R = 0.030$ and $R_w = 0.075$ for **5**, and $R = 0.035$ and $R_w = 0.030$ for **7**. Selected bond distances and angles are listed in Table 2. Tables of thermal parameters and selected final atomic coordinates are given in the Supporting Information.

Acknowledgment. We would like to thank the National Science Council of Taiwan, the Republic of China, for support.

Supporting Information Available: Plot of VT NMR spectra of **5** in CD₂Cl₂ and CD₃CN, and of **3** and **5** in CDCl₃; tables of atomic coordinates, crystal and intensity collection data, anisotropic thermal parameters, and bond distances, and bond angles for **2**, **4**, **5**, and **7**. This material is available free of charge via the Internet at <http://pubs.acs.org>.

OM0207156

(16) Gabe, E. J.; Lee, F. L.; Lepage, Y. *Crystallographic Computing 3*; Sheldrick, G. M., Kruger, C., Eds.; Clarendon Press: Oxford, England, 1985; p 167.

(17) *International Tables for X-ray Crystallography*; Reidel: Dordrecht, The Netherlands, 1974; Vol. IV.